

Figure 2. Dependence of the photochemical quantum yield on the luminescent lifetime of the Tb(thd)<sub>3</sub>-alcohol adduct.

likely is the photodissociation process. This correlation may imply that the photoreactive state is f-f in nature, but this conclusion is not in accord with our other results. If the <sup>5</sup>D<sub>4</sub> level of Tb(III) is indeed the photoactive state, then one would expect to observe appreciable photoreaction at 365 nm as well as at 311 nm since both excitation wavelengths are very efficient at populating the <sup>5</sup>D<sub>4</sub> state. It is possible that the photochemistry occurs via a low-lying ligand state, which can exchange energy with the <sup>5</sup>D<sub>4</sub> state; the longer the lifetime of the <sup>5</sup>D<sub>4</sub> state, the more opportunity there would be for photodissociation to occur from

the chelate level.<sup>15</sup> It should be noted that we have determined that the Tb(III) lifetime of Tb(thd)<sub>3</sub> in *sec*-butyl alcohol is 700 μs and that the lifetime in *tert*-butyl alcohol is 625 μs.

The results presented in this paper demonstrate that lanthanide β-diketonate complexes are capable of exhibiting photochemical reactions and indicate a need for further study. The evidence we have presented indicates that the degree of photodissociation depends on two factors: the interaction of the complex with the solvent and the actual lifetime of the metal excited state. We are currently pursuing studies designed to develop these proposals in a more detailed fashion.

*Acknowledgment.* This work was supported by a Cottrell grant from the Research Corporation (No. 8926) and by the National Science Foundation (Grant CHE 78-03402).

## References and Notes

- (1) A. P. B. Sinha in "Spectroscopy in Inorganic Chemistry", Vol. II, C. N. R. Rao and J. R. Ferraro, Eds., Academic Press, New York, 1971.
- (2) L. I. Anikina and A. V. Karyakin, *Russ. Chem. Rev. (Engl. Transl.)*, **39**, 673 (1970).
- (3) (a) T. J. Sworski, *J. Phys. Chem.*, **67**, 2858 (1963); (b) R. A. Sheldon and J. K. Kochi, *J. Am. Chem. Soc.*, **90**, 6688 (1968); (c) R. W. Matthews and T. J. Sworski, *J. Phys. Chem.*, **79**, 681 (1975).
- (4) (a) D. D. Davis, K. L. Stevenson, and G. K. King, *Inorg. Chem.*, **16**, 670 (1977); (b) T. Donohue, *J. Chem. Phys.*, **67**, 5402 (1977); (c) M. Brandys and G. Stein, *J. Phys. Chem.*, **82**, 852 (1978).
- (5) T. Donohue, *J. Am. Chem. Soc.*, **100**, 7411 (1978).
- (6) K. J. Eisenbraun and R. E. Slevers, *Inorg. Synth.*, **11**, 94 (1968).
- (7) J. G. Calvert and J. N. Pitts, "Photochemistry", Wiley, New York, 1966, pp 732-735.
- (8) Reference 7, pp 783-786.
- (9) H. G. Brittain, *Inorg. Chem.*, **17**, 2762 (1978).
- (10) M. L. Bhaumik, *J. Chem. Phys.*, **40**, 3711 (1964).
- (11) J. N. Demas, E. W. Harris, and R. P. McBride, *J. Am. Chem. Soc.*, **99**, 3547 (1977).
- (12) H. G. Brittain, *J. Chem. Soc., Dalton Trans.*, 1187 (1979).
- (13) T. Moeller, D. F. Martin, L. C. Thompson, R. Ferrus, G. R. Feistel, and W. J. Randall, *Chem. Rev.*, **65**, 1 (1965).
- (14) H. G. Brittain and F. S. Richardson, *J. Chem. Soc., Faraday Trans. 2*, **73**, 545 (1977).
- (15) The author is indebted to one of the referees for this suggestion.

## Formation of Ion Pairs in Rubidium-Tetrahydrofuran Crown Ether Solutions<sup>1</sup>

U. Ellav<sup>2</sup> and Halm Levanon<sup>\*3</sup>

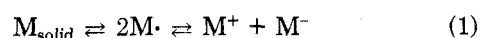
Department of Physical Chemistry, The Hebrew University, Jerusalem, Israel, and the Radiation Laboratory, University of Notre Dame, Notre Dame, Indiana 46556 (Received March 8, 1979; Revised Manuscript Received August 20, 1979)

Publication costs assisted by the Division of Basic Energy Sciences, U.S. Department of Energy

The effect of dicyclohexyl-18-crown-6 (CR) on the transient species formed in irradiated solutions (pulse radiolysis) of THF saturated with rubidium metal was investigated. Analysis of the kinetics and spectra of the transients reveals that, in addition to the metal anion Rb<sup>-</sup>, the solvated monomer Rb<sup>•</sup>, and the solvated electron e<sub>s</sub><sup>-</sup>, a new species attributed to an ion pair of the type (RbCR<sup>+</sup>,e) is formed in solutions containing CR. This species is characterized by its absorption spectrum and its formation by a second-order process, Rb<sup>•</sup> + CR ⇌ (RbCR<sup>+</sup>,e). The absorption spectrum of Rb<sup>•</sup> is peaked around 1250 nm and that of (RbCR<sup>+</sup>,e) around 1800 nm, with molar extinction coefficients being 2.4 × 10<sup>4</sup> M<sup>-1</sup> cm<sup>-1</sup> and 2.8 × 10<sup>4</sup> M<sup>-1</sup>, respectively. It is concluded that the addition of CR to THF is equivalent to the increase in the donor number of the solvent in which the alkali metal is dissolved.

### Introduction

The chemical equilibrium of alkali metals dissolved in nonpolar solvents is commonly described by the set of reactions<sup>4</sup>



These reactions strongly depend on the specific metal as well as on environmental factors such as temperature

and/or solvent. The anionic species  $M^-$  is the only one which is present at a sufficiently high concentration and thus can be detected in its ground state by optical spectroscopy. Therefore, other spectroscopic methods like ESR,<sup>5-9</sup> laser<sup>10</sup> or flash photolysis,<sup>11</sup> and pulse radiolysis<sup>12-14</sup> have been applied to study the above equilibria and to differentiate between the chemical constituents either in their ground state or as transients.

Reactions 1-3 as stated above do not take into account the inherent properties of the solvents in affecting the stoichiometry of the chemical species. Specifically, this scheme does not include the possible existence of both the loose ion pair ( $M^+, e^-$ ) and the solvated monomer ( $M\cdot$ ).<sup>15</sup> These two species have been identified in pulse radiolysis experiments, and evidence for the dynamic equilibrium ( $M^+, e^- \rightleftharpoons M\cdot$ ) has been proposed.<sup>16</sup> These authors show that in poor chelating solvents, e.g., THF, one species predominates, namely, the solvated monomer, whereas in triglyme, for example, the loose ion pair is exclusively obtained. Mixed solvents are the proper media for obtaining both species. The existence of loose and tight ion pairs, with different spectral properties, has been proposed also in the analysis of ESR spectra<sup>5,17</sup> and, like the pulse radiolysis experiments, it was found to be solvent and temperature dependent.

The addition of chelating agents like crown ethers (CR) is considered to affect equilibria 1-3 by the addition of the reaction



having a high equilibrium constant,  $K_4 \approx 10^9 M^{-1}$ , for  $M = Na$ .<sup>18</sup> This reaction shifts the total equilibria 1 and 3 to the right, whereas equilibrium 2 is unaffected as long as  $M_s$  is in contact with the solvent.

In the present study we demonstrate that the addition of CR to a solution of Rb-THF cannot be described solely in terms of the added reaction 4 but involves as well a stoichiometric change in the constituents which participate in the above reactions, namely, formation of different types of constituents, e.g., ( $RbCR^+, e^-$ ) and  $Rb\cdot$ , respectively. The former species bears some relation to the loose pair ( $M^+, e^-$ ), whereas the latter species is identified with the solvated monomer  $M\cdot$ . These species which differ in their stoichiometry undergo a dynamic equilibrium which depends on the concentration of the chelating agent CR.

### Experimental Section

A solution containing THF and rubidium metal in excess was prepared in an apparatus<sup>19</sup> modified to our purposes as shown in Figure 1. The metal was separately distilled via a sidearm Pyrex tubing with three constrictions, and the solvent was vacuum distilled into flask A from a stock solution of THF kept on Na-K alloy. When CR was required in the experiment, it was kept under vacuum and separated from the main apparatus by a breakseal. Before each experiment the main apparatus was sealed off, and the experiment was carried out by flowing the solution through the reaction cell as is described in the caption to Figure 1. Experiments were carried out in a closed-flow system, resulting in the deterioration of the solution because of the irradiation. To ensure reproducibility of the results, measurements were repeated after 50 pulses of irradiation. The solution was discarded after deviations of more than 10% in the results were noticed. The detector used in these experiments, which covered the entire spectral range 600-2200 nm, was an In-Sb Judson J-10, cooled to liquid  $N_2$  temperature (bandwidth  $\leq 10$  MHz). The kinetic spectrophotometric experiments were carried out with signal averaging by using the computer-controlled

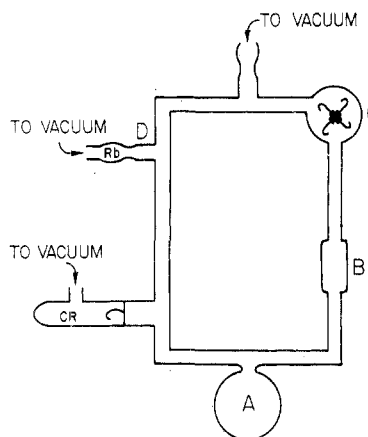
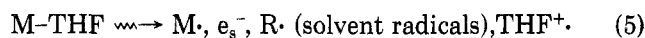


**Figure 1.** Closed-flow system apparatus for irradiated solutions of Rb-THF: A is 100-mL flask into which THF was distilled; B is the spectrophotometric (1-cm pathway) cell; C is a rotator, made of glass, adapted to the form shown. A bar magnet was built into one of the glass arms, and with an external rotating magnet the glass rotator circulated the solution. Rubidium metal was distilled into the main apparatus via the side arm D.

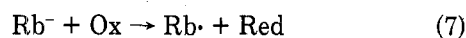
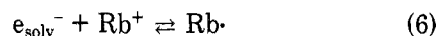
pulse radiolysis apparatus described previously.<sup>20,21</sup> Ground-state spectra were taken with conventional evacuated samples by using a Cary 14 spectrometer. All experiments were performed at room temperature.

### Results and Discussion

Irradiation of solutions of THF saturated with rubidium metal results in the following species in the primary radiolytic process



These short-lived intermediates react with the alkali metal species according to the following fast and slower reactions, respectively.



(We designate the rate constant for a forward and a backward reaction as  $k_1$  and  $k_{-1}$ , respectively.) The forward reaction in equilibrium 7 is observed as a bleach process, because the formation of the monomer  $Rb\cdot$  is accompanied by the decrease in absorption of  $Rb^-$ . The bleaching of  $Rb^-$  is caused by the reaction of this anion with different oxidizing agents (Ox) like  $THF^+$  and solvent radicals ( $R\cdot$ ). Typical kinetic curves describing the forward reactions 6 and 7 are shown in Figure 2. Figure 2a shows the formation of  $Rb\cdot$ , at  $\lambda = 1350$  nm, via reaction 6, which is followed by a slower process attributed to reaction 7. Figure 2b shows the bleaching process of  $Rb^-$  at a typical wavelength where this anion absorbs,  $\lambda = 925$  nm.

The rate constant  $k_6$  can be determined either from the fast-buildup component (shown in Figure 2a) or alternatively from the decay of the absorption of  $e_s^-$  in the spectral region  $\lambda > 1800$  nm. In both regions the fast formation (or decay) curves were obtained in a poor signal-to-noise ratio, resulting in a low accuracy in the determination of the pseudo-first-order rate constant,  $k_6' = k_6[Rb^+] + k_{-6}$ .

As more than one oxidizing agent is involved in reaction 7, one should expect more than one rate constant for the forward reaction,  $k_7$ . In our experiments, however, we measure a single half-lifetime from the exponential curves (Figure 2b). The concentration of the metal anion  $M^-$  was determined from its absorption in the ground state. In our experiments,  $[Rb^-] = (2-3) \times 10^{-6} M$ , and, since the bleach is far from being complete, it is obvious that  $[THF^+] +$

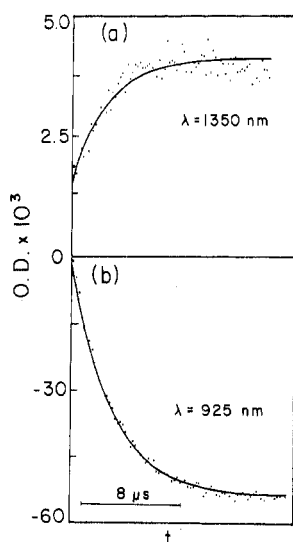


**Figure 2.** Typical curves describing the kinetic processes as given by eq 6 and 7 in the text. (a) The slow process to produce  $\text{Rb}\cdot$  (reaction 7) starts after the fast process to produce  $\text{Rb}\cdot$  (reaction 6) is completed. (b) The bleach process of  $\text{Rb}^-$  (reaction 7). Full lines are the best-fit curves to a first-order process.

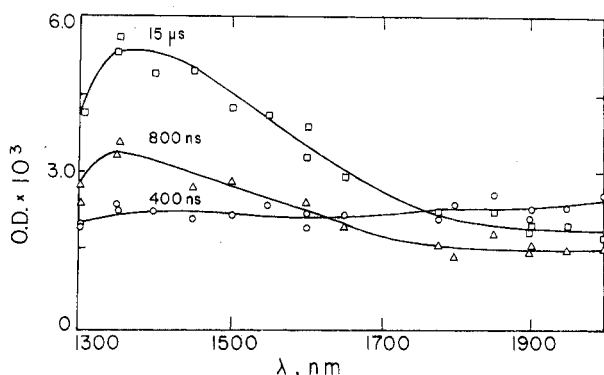


**Figure 3.** Transient absorption spectra of an irradiated solution of  $\text{Rb}\cdot$ -THF at different times shown on each trace. No correction to the spectra due to superposition of different absorption has been made.

$[\text{R}\cdot] < [\text{Rb}^-]$ . Since the concentration of  $\text{R}\cdot$  exceeds that of  $\text{THF}^+$  by an order of magnitude,<sup>22</sup> the observed pseudo-first-order kinetics of eq 7 is attributed to the reaction with  $\text{R}\cdot$ . It is reasonable to assume that the reaction with  $\text{THF}^+$ , which is much faster escapes detection because it has been completed. We determine, therefore, that  $k_7 = (1.4 \pm 0.2) \times 10^{10} \text{ M}^{-1} \text{ s}^{-1}$  for the reaction with  $\text{R}\cdot$ . The result for  $k_7$  is very similar to the corresponding reaction rate obtained when potassium metal was dissolved in THF.<sup>23</sup>

Transient absorption spectra, at three different times in the region 1300–2000 nm, are shown in Figure 3. At 400 ns after the pulse, the absorption slightly increases on increasing  $\lambda$ . At 800 ns after the pulse, the absorption around 1300 nm still increases, whereas at the same time the absorption around 1800 nm decreases. At longer times, 15  $\mu\text{s}$  after the pulse, a further growth in the absorption is observed in both regions but is much more pronounced in the vicinity of 1250–1300 nm.

These temporal changes in the absorption spectra are interpreted in terms of reactions 6 and 7 under the assumption that the absorption in this wavelength region is due to  $\text{Rb}\cdot$  ( $\lambda_{\text{max}} \approx 1250 \text{ nm}$ ) and to the known absorption of the solvated electron,  $e_s^-$  in THF ( $\lambda_{\text{max}} \approx 2100 \text{ nm}$ ).<sup>23,24</sup> In times shorter than 800 ns, when reaction 7 has not yet started, the changes in the absorption occur via reaction 6. The solvated monomers,  $\text{Rb}\cdot$ , increase in concentration

while  $e_s^-$  decreases toward equilibrium. In times longer than 1  $\mu\text{s}$ , reaction 7 starts to be effective in contributing  $\text{Rb}\cdot$ ; hence, the absorption around 1300 nm is increased accordingly. These two contributions at different time scales are clearly demonstrated in Figure 3. It should be noted that wavelengths above 1800 nm the main contribution to the absorption is from the solvated electron,  $e_s^-$ , which has not completely disappeared but rather has accomplished an equilibrium concentration according to reaction 6.

From the experimental data together with the already known spectra of  $e_s^-$  in THF,<sup>23,24</sup> we determined the spectral line shape of  $\text{Rb}\cdot$  and  $\text{Rb}^-$  in THF. The line shape of the former species was determined from the bleaching process (Figure 2b) at a wavelength range of 650–1100 nm. This spectral line shape of  $\text{Rb}\cdot$  is identical with the ground-state spectrum of a  $\text{Rb}\cdot$ -THF solution, and its maximum lies around 955 nm at room temperature. Its main features are very similar to those reported previously for the ground-state spectrum of  $\text{Rb}\cdot$ -methylamine solutions.<sup>11</sup> Once the absorption spectrum of  $\text{Rb}\cdot$  is known, it is possible to determine the absorption spectrum of  $\text{Rb}^-$ . We attribute the temporal change in the absorption between 800 ns and 15  $\mu\text{s}$  to the corresponding increase in concentration of  $\text{Rb}\cdot$  via reaction 7. In other words, in this time interval the equilibrium concentration of  $e_s^-$  has not been considerably changed. Therefore, we can calculate the extinction coefficient of  $\text{Rb}\cdot$  by using the following considerations. If one takes into account that reactions 6 and 7 occur on different time scales,  $0 < t < 800 \text{ ns}$  and  $800 \text{ ns} < t < 15 \mu\text{s}$ , respectively, then the buildup concentration of  $\text{Rb}\cdot$ , the decay of  $e_s^-$ , and the bleaching of  $\text{Rb}^-$  are given respectively by

$$\begin{aligned} [\text{Rb}\cdot] &= [\text{Rb}\cdot]_0^6 [1 - e^{-k_6 t}] + [\text{Rb}\cdot]_0^7 [1 - e^{-k_7 t}] \\ [e_s^-] &= \{[e_s^-]_{\text{initial}} - [e_s^-]_0^6\} e^{-k_6 t} + [e_s^-]_0^6 \\ [\text{Rb}^-] &= [\text{Rb}^-]_0^7 [1 - e^{-k_7 t}] \end{aligned} \quad (8)$$

where  $[ ]_0^i$  is the concentration of the corresponding species at times  $t \gg 1/k_i'$  ( $i = 6, 7$ ), and  $k_6'$  and  $k_7'$  are the pseudo-first-order rate constants for reactions 6 and 7. In the spectral region where  $\text{Rb}\cdot$  and  $e_s^-$  are the only absorptive species, the time-dependent observed absorption, which reflects changes in the corresponding concentration, can be expressed by utilizing eq 8 and  $\text{OD}_{\text{obsd}}(t) = \text{OD}_{\text{Rb}\cdot}(t) + \text{OD}_{e_s^-}(t)$ . In the time interval of 1–15  $\mu\text{s}$ , the contribution of  $\text{OD}_{e_s^-}$  and  $\text{OD}_{\text{Rb}\cdot}$ , due to reaction 6, is calculated from the plateau region in the absorptions of  $\text{Rb}\cdot$  and  $e_s^-$  after reaction 6 is complete,  $t = 1 \mu\text{s}$ . Their values are  $\text{OD}_{e_s^-}(1 \mu\text{s}) = \epsilon_{e_s^-} [e_s^-]_0^6$  and  $\text{OD}_{\text{Rb}\cdot}(1 \mu\text{s}) = \epsilon_{\text{Rb}\cdot} [\text{Rb}\cdot]_0^6$ . Since  $\Delta[\text{Rb}^-] = -\Delta[\text{Rb}\cdot]$ , which is valid in the time interval where reaction 7 occurs, we calculate  $\epsilon_{\text{Rb}\cdot}$  via the relation  $[\text{OD}_{\text{obsd}}(t) - \text{OD}_{e_s^-}(1 \mu\text{s}) - \text{OD}_{\text{Rb}\cdot}(1 \mu\text{s})] / \epsilon_{\text{Rb}\cdot} = \text{OD}_{\text{Rb}\cdot}(t) / \epsilon_{\text{Rb}\cdot}$ ; in our calculations we chose  $\lambda_1 = 955 \text{ nm}$ .

In the region where overlap between the bleach and absorption spectra exists,  $1350 \text{ nm} > \lambda > 1000 \text{ nm}$ , the analysis described above is not adequate because  $\text{OD}_{\text{Rb}\cdot}$  and  $\text{OD}_{\text{Rb}^-}$  cannot be determined separately (the absorption due to  $e_s^-$  in this wavelength region is negligible). In order to decompose the observed optical density into its two components, we attribute the partial recovery process, which can be experimentally observed (Figure 4), to reaction 9. This recovery occurs on a long time scale (15



$\mu\text{s} < t < 400 \mu\text{s}$  after the pulse) and obeys pseudo-first-order kinetics from which the second-order rate constant  $k_9 = 5.7 \times 10^{10} \text{ M}^{-1} \text{ s}^{-1}$  was determined. In this time in-

TABLE I: Reaction Rates, Equilibrium Constants, and Molar Extinction Coefficients for Reactions and Species in M-THF and M-THF-CR Solutions

reactions and $\epsilon^{\max}$	rate constants	Na, M	K, M	Rb, M	Cs, M
$e_s^- + M^+ \rightleftharpoons M\cdot$	$k_6^a$	$7.8 \times 10^{11} d, e$	$4.6 \times 10^{11} e, f$	$(6 \pm 2) \times 10^{11}$	$\sim 5 \times 10^{11} e$
$\epsilon_{Rb\cdot}^{\max} = (2.4 \pm 0.4) \times 10^4 M^{-1} cm^{-1}$	$k_{-6}^b$	$0.8 \times 10^5 f$	$1.6 \times 10^5 f$	$(6 \pm 2) \times 10^5$	
$M^- + THF^+ \cdot \rightarrow M\cdot + THF$	$K_6^c$	$9.8 \times 10^4 f$	$2.9 \times 10^6 f$	$(1.0 \pm 0.3) \times 10^6$	
$M^- + R\cdot \rightarrow M\cdot + \text{products}$	$k_7^a$		$1.0 \times 10^{11} f$	$> 5 \times 10^{10}$	
$M\cdot + e_s^- + M^-$	$k_7^a$		$2.0 \times 10^{10} f$	$(1.4 \pm 0.2) \times 10^{10}$	
$\epsilon_{Rb^-}^{\max} = (2 \pm 0.4) \times 10^5 M^{-1} cm^{-1}$	$k_9^a$	$1 \times 10^{10} f$	$1 \times 10^{10} f$	$(5.7 \pm 0.7) \times 10^{10}$	

<sup>a</sup> In units of  $M^{-1} s^{-1}$ . <sup>b</sup> In units of  $s^{-1}$ . <sup>c</sup> In units of  $M^{-1}$ . <sup>d</sup> Reference 12. <sup>e</sup> Reference 14. <sup>f</sup> Reference 23.

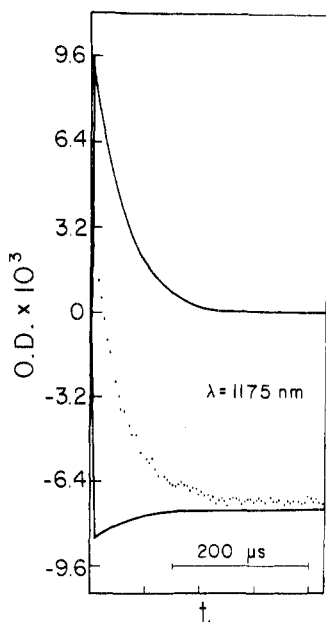


Figure 4. An experimental curve taken in a region where an overlap between bleach and absorption occurs (dotted line). The solid lines are the calculated two components: in the negative scale, the bleach and recovery process; in the positive scale, the absorption and its decay process.

terval the concentration of  $Rb^-$  through the recovery process will be given by eq 10, where  $\alpha$  defines the extent  $[Rb^-] = [Rb^-]_0^7 [1 - e^{-k_7' t}] [\alpha + (1 - \alpha) e^{-k_9' t}] \approx$

$$[Rb^-]_0^7 [\alpha + (1 - \alpha) e^{-k_9' t}] \quad (10)$$

of recovery ( $[Rb^-] \gg [e_s^-]$ ) and is predetermined from the recovery curves at wavelengths where  $Rb^-$  is the only species which absorbs, i.e.,  $\alpha = [Rb^-]_{t=\infty} / [Rb^-]_{t=15\mu s}$ , and  $k_9'$  is the pseudo-first-order rate constant for reaction 9. Notice that for  $t \geq 15 \mu s$ ,  $k_7' t \gg 1$  and  $[Rb^-]_0^7$  serves as the initial condition for the recovery process. On the other hand, the decay process of  $Rb\cdot$  in this time interval (reaction 9) obeys the same rate law as that of the recovery process. The expression for the time-dependence concentration of  $Rb\cdot$  is obtained by the same consideration given above in the derivation of eq 10.

$$[Rb\cdot] \approx \{ [Rb\cdot]_0^6 + [Rb\cdot]_0^7 \} e^{-k_9' t} \quad (11)$$

The observed time-dependence optical absorption in the overlapping region will be given in terms of eq 10 and 11 and  $OD_{\text{obsd}}(t) = OD_{Rb^-}(t) + OD_{Rb\cdot}(t)$ . Knowing  $k_9'$ , together with the observed optical absorption at  $t = \infty$  and  $t = 15 \mu s$ , enables one to calculate separately  $OD_{Rb^-}(t)$  and  $OD_{Rb\cdot}(t)$  and thus to decompose the experimental curve into its two components. By employing now the same procedure as in the nonoverlapping region, we calculate  $\epsilon_{Rb^-}^{\lambda}$ .

In Figure 4 we demonstrate how the experimental curve taken at 1175 nm is resolved into its two components.

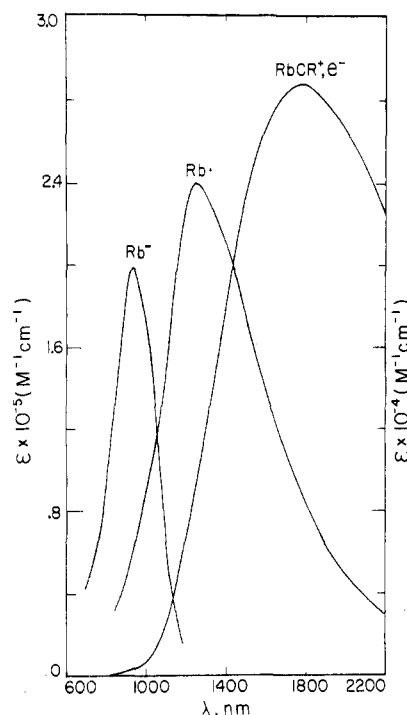
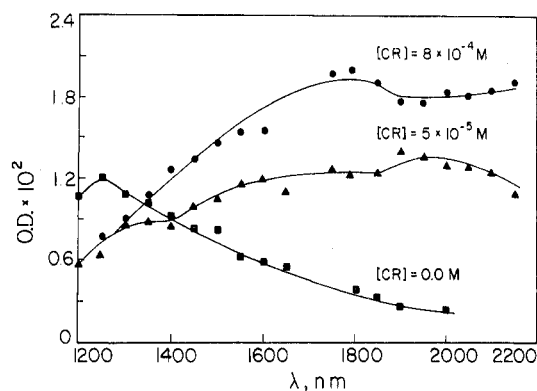


Figure 5. Calculated absorption spectra of the anion,  $Rb^-$ , the solvated monomer,  $Rb\cdot$ , and the ion pair,  $(RbCR^+ \cdot e^-)$ , in THF solutions. The latter spectrum is the calculated one and was obtained similarly to that of  $Rb\cdot$  (see text). The left-hand abscissa corresponds to  $Rb^-$  and the right-hand one to  $Rb\cdot$  and  $(RbCR^+ \cdot e^-)$ .

Figure 5 shows the calculated spectra, employing the above procedure, of the anion  $Rb^-$  and that of the solvated monomer  $Rb\cdot$ . It is evident that the molar extinction coefficient for  $Rb^-$  is larger by an order of magnitude than that of  $Rb\cdot$ ,  $\epsilon_{Rb^-}^{\max} = (2.0 \pm 0.4) \times 10^5 M^{-1} cm^{-1}$ ,  $\epsilon_{Rb\cdot}^{\max} = (2.4 \pm 0.4) \times 10^4 M^{-1} cm^{-1}$ .

From the absorption spectra determined in the present study together with the already known spectra of  $e_s^-$ ,<sup>23,24</sup> and assuming that  $[Rb^-] \approx [Rb^+]$ , we could evaluate the equilibrium constant,  $k_6 = (1.0 \pm 0.2) \times 10^6 M^{-1}$ . Knowing the pseudo-first-order rate, we calculated  $k_6'$  for the forward and reverse reaction 6 as  $k_6 = (6.0 \pm 2.0) \times 10^{11} M^{-1} s^{-1}$  and  $k_{-6} = (6.0 \pm 2.0) \times 10^5 M^{-1} s^{-1}$ , respectively. These results are consistent with those found for other alkali metals and are compared in Table I.

To check the results given above, we calculated the oscillator strength  $f$  for both  $Rb^-$  and  $Rb\cdot$  by evaluating the integral  $4.3 \times 10^{-9} \int \epsilon_\nu d\nu$ . The values for  $f = 2.2$  and 0.46 for  $Rb^-$  and  $Rb\cdot$ , respectively. This value for  $Rb^-$  is reasonable if the absorption spectrum of  $Rb^-$  originates from the electronic excitation of two equivalent electrons in the anionic species. A very similar value for  $f$  has been reported for  $Na^-$  in ethylenediamine solutions,<sup>25</sup> whereas a somewhat higher value ( $f = 0.52$ ) is calculated for  $Cs^-$  from its absorption in THF.<sup>14</sup>



**Figure 6.** Transient absorption spectra of irradiated solutions of Rb-THF with different CR concentrations. The solid lines are the calculated spectra (see text). The OD values for  $[CR] = 5 \times 10^{-5} M$ ;  $OD_1^0 = 0.2 \times 10^{-2}$ ,  $OD_2^0 = 1.2 \times 10^{-2}$ ,  $OD_3^0 = 0.23 \times 10^{-2}$ . For  $[CR] = 8 \times 10^{-4} M$ ;  $OD_1^0 = 0.1 \times 10^{-2}$ ,  $OD_2^0 = 1.9 \times 10^{-2}$ ,  $OD_3^0 = 0.45 \times 10^{-2}$ .

**Rb-THF-CR.** The addition of the complexing agent CR substantially affects the experimental observations. This is reflected mainly by a change in the transient absorption spectrum in the region 1300–2100 nm. In Figure 6 we show the transient absorption spectra, taken at the plateau region of the kinetic curves for solutions of Rb-THF containing  $5 \times 10^{-5} M$  CR ( $\sim 3 \mu s$  after the pulse) and  $8 \times 10^{-4} M$  CR ( $\sim 1 \mu s$  after the pulse). For comparison we also show the transient absorption spectrum in the same wavelength region for Rb-THF solution without CR added. The experimental points, in all three cases, in the region where overlap between the bleach process and the absorption occurs (1200–1350 nm) were corrected according to the procedure described above.

Inspection of Figure 6 shows that the absorption around 1300 nm (where Rb $\cdot$  absorbs) is slightly affected by the addition of CR. On the other hand, two additional broad absorptions having peaks around 1800 and 2100 nm are observed. These absorptions are formed simultaneously and increase monotonically with increasing CR concentration. The times in which these transient spectra are formed correspond exactly to the times in which the bleaching process occurs (cf. reaction 7). This implies that the new species which is responsible for the absorption at 1800 nm originates from Rb $\cdot$  and is not the solvated electron  $e_s^-$  or the solvated monomer Rb $\cdot$ . We thus attribute the absorption around 1800 nm to an additional type of species which consists of an electron and a cation, as will be discussed below. The changes in the absorptions above 1800 nm are due to an increase in the concentration of the solvated electron. Because the solvated electron in this case is not observed on a submicrosecond time scale, contrary to the results described in the previous section, this production of electrons must originate from a secondary reaction. In order to calculate the absorption spectrum of the additional species, formed in Rb-THF-CR solutions, it is essential to decompose each of the experimental absorption spectra given in Figure 6 into three separate components.

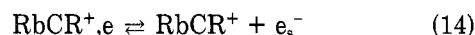
The solid lines in Figure 6 are the calculated curves which have been determined by assigning a Gaussian shape for each component, i.e.,

$$OD_T = \sum_{i=1}^3 OD_i^0 \exp \left[ - \left( \frac{\nu - \nu_i^0}{\frac{1}{2} \Delta \nu_i} \right)^2 \times \ln 2 \right] \quad (12)$$

where  $OD_T$  is the calculated total absorption;  $\nu_i^0$  ( $i = 1, 3$ ) are the frequencies corresponding to the absorption peaks of the three species, namely, Rb $\cdot$ , "new" species, and  $e_s^-$ ,

respectively.  $OD_i^0$  are the absorption values at the maxima. The value for  $\nu_1^0$  was determined in Rb-THF solution:  $\nu_1^0 = 8000 \text{ cm}^{-1}$  and  $\frac{1}{2} \Delta \nu_1 = 1900 \text{ cm}^{-1}$  (Figures 5 and 6);  $\nu_3^0$  and  $\frac{1}{2} \Delta \nu_3$  were taken<sup>24,26</sup> as 4545 and 600  $\text{cm}^{-1}$ , respectively;  $\nu_2^0$  and  $OD_2^0$  ( $i = 1, 3$ ) were determined by a best-fit analysis according to expression 10. The value for  $\nu_2^0$  was found to be 5714  $\text{cm}^{-1}$ , and the half-widths at half-heights,  $\frac{1}{2} \Delta \nu_2 = 1850 \text{ cm}^{-1}$ . This analysis indicates that the ratios between the absorptions at 1250, 1784, and 2100 nm, namely,  $OD_1^0:OD_2^0:OD_3^0$ , decrease on increasing the CR concentration, which is reflected by a red shift of the spectrum. The calculated absorption spectra of the "new" species is shown in Figure 5.

These observations cannot be accounted for in terms of equilibria 1–4. It is obvious that a new stoichiometric species, not included in the basic reactions above, has been formed upon the addition of CR. We propose, therefore, the following processes which include the participation of CR in the following reactions:



These two reactions occur in a period of 300 ns, which is within the bleach process. The formation of the new absorption around 1800 nm, which is red shifted in comparison to the absorption of Rb $\cdot$ , is consistent with the production of an ion pair of the type (RbCR $^+$ , e). Additional support for the existence of (RbCR $^+$ , e) is from previous ESR studies in which this species has been suggested.<sup>8</sup> The calculated molar extinction coefficient,  $\epsilon_{RbCR^+, e}^{\max} = (2.8 \pm 0.5) \times 10^4 \text{ M}^{-1} \text{ cm}^{-1}$ , is of the same order as that calculated for  $\epsilon_{Rb\cdot}^{\max}$ .

Comparing the results obtained in this study for Rb-THF solutions containing the chelating agent CR to those obtained with alkali metals in chelating solvents is quite interesting. The only available data are with sodium salts, Na $^+$ BPh $_4^-$  and NaAlH $_4$ , dissolved in DME, diglyme, and triglyme, as studied by Seddon et al.<sup>16</sup> They demonstrated that the ratio between the loose and tight ion pairs increases on increasing the chelating ability of the solvents or alternatively by decreasing the temperature. In the present work we demonstrate that the addition of small quantities of CR to THF, a solvent having a relatively low dielectric constant, changes the ratio between the (RbCR $^+$ , e) and Rb $\cdot$  in a similar way as to increase the chelating ability of the solvent. In addition we have demonstrated that the addition of CR results in species in which the electron is loosely bonded to the cation RbCR $^+$ . Our findings may imply that the macrodielectric constant has a secondary effect and that the coordination power is the dominant factor in the determination of the above ratio.

**Acknowledgment.** We are grateful to Professors R. H. Schuler and R. W. Fessenden and to Dr. P. Neta for stimulating discussions while the authors were visiting the Radiation Laboratory, University of Notre Dame.

## References and Notes

- The work described herein was supported by the Office of Basic Energy Sciences of the Department of Energy, U.S.A., and by the Israel Commission of Basic Research. This is document No. 1982 from the Notre Dame Radiation Laboratory.
- Summer Student at the University of Notre Dame (1978) and in partial fulfillment of the requirements for the Ph.D. degree at the Hebrew University of Jerusalem, Israel.
- The Hebrew University. Visiting Professor at the University of Notre Dame, Summer 1978.
- For a recent review see, e.g., J. L. Dye in "Multidentate Macrocyclic Molecules", J. J. Christensen and R. M. Izatt, Eds., Wiley-Interscience, New York, in press.

- (5) R. Catterall, J. Slater, and M. C. R. Symons, *Can. J. Chem.*, **55**, 1979 (1977).
- (6) T. R. Tuttle, Jr., *J. Phys. Chem.*, **79**, 3071 (1975).
- (7) S. H. Glarum and J. H. Marshall, *J. Chem. Phys.*, **52**, 5555 (1970).
- (8) A. Friedenberg and H. Levanon, *J. Phys. Chem.*, **81**, 766 (1977).
- (9) U. Ellav and H. Levanon, *Chem. Phys. Lett.*, **55**, 369 (1978).
- (10) D. Huppert, Ph. Avauries, and P. M. Rentzepis, *J. Phys. Chem.*, **82**, 2282 (1978).
- (11) M. Ottolenghi, K. Bar-Eli, and H. Linschitz, *J. Chem. Phys.*, **43**, 206, 1965.
- (12) B. Bockrath and M. Dorfman, *J. Phys. Chem.*, **77**, 1002 (1973).
- (13) G. A. Salmon and W. A. Seddon, *Chem. Phys. Lett.*, **24**, 366 (1974).
- (14) For a general survey on pulse radiolysis experiments of alkali metals see J. W. Fletcher and W. A. Seddon, *J. Phys. Chem.*, **79**, 3055 (1975), and references therein.
- (15) For a general concept of loose and tight ion pairs between alkali metal cations and anionic hydrocarbons, see M. Szwarc, in "Ions and Ion Pairs in Organic Reactions", Vol. I, M. Szwarc, Ed., Wiley-Interscience, New York, 1972.
- (16) W. A. Seddon, J. W. Fletcher, F. C. Sopchysyn, and R. Catterall, *Can. J. Chem.*, **55**, 3356 (1977).
- (17) R. Catterall and P. P. Edwards, *J. Phys. Chem.*, **79**, 3010 (1975).
- (18) J. L. Dye, C. W. Andrews, and S. E. Mathews, *J. Phys. Chem.*, **79**, 3065 (1975).
- (19) G. Foldiak and R. H. Schuler, *J. Phys. Chem.*, **82**, 2756 (1978).
- (20) L. K. Patterson and J. Lillie, *Int. J. Radiat. Phys. Chem.*, **6**, 129 (1974).
- (21) R. H. Schuler, P. Neta, H. Zemel, and R. W. Fessenden, *J. Am. Chem. Soc.*, **98**, 3823 (1976).
- (22) The R<sup>-</sup> concentration  $5 \times 10^{-7}$  M was determined by knowing to what extent Rb<sup>-</sup> was bleached together with the known concentration of THF<sup>+</sup>  $\approx 4.3 \times 10^{-8}$  M.<sup>23</sup>
- (23) G. A. Salmon, W. A. Seddon, and J. W. Fletcher, *Can. J. Chem.*, **52**, 3259 (1974).
- (24) L. M. Dorfman, F. Y. Jon, and R. Wageman, *Ber. Bunsenges. Phys. Chem.*, **75**, 681 (1971).
- (25) J. L. Dye and L. H. Feldman, *Rev. Sci. Instrum.*, **37**, 154 (1966).
- (26) The absorption spectrum of e<sub>s</sub><sup>-</sup> is asymmetrical; we therefore take the value for  $1/2\Delta\nu_3$ , in eq 12, from the "red tail" of the spectrum attributed to the e<sub>s</sub><sup>-</sup> in the presence of cryptate. See, e.g., J. L. Dye, in "Electrons in Fluids", J. Jortner and R. R. Kestner, Eds., Springer-Verlag, New York, 1973, p 83.

## Excited State Reactivity of Aza Aromatics. 9. Fluorescence and Photoisomerization of Planar and Hindered Styrylpyridines

G. Bartocci, U. Mazzucato,\* F. Masetti,

*Istituto di Chimica Fisica, Università di Perugia, I-06100 Perugia, Italy*

and G. Galiazzi

*Istituto di Chimica Organica, Università di Padova, I-35100 Padova, Italy (Received August 7, 1979)*

*Publication costs assisted by the Consiglio Nazionale delle Ricerche (Roma)*

The effect of methyl substitution at the ethylenic bridge on the fluorescence and trans  $\rightarrow$  cis photoisomerization of styrylpyridines (StP's) has been investigated. As compared with the unsubstituted planar olefins, steric hindrance modifies the shape of the potential energy barrier for photoisomerization. The hindered compounds show a marked decrease in the fluorescence quantum yield. A parallel decrease in the photoreaction quantum yield has been observed for the  $\alpha$ -methyl derivatives of stilbene and 3-StP. Temperature and solvent effects on planar and hindered StP's give interesting information on the intramolecular rotation in excited azastilbenes and its competition with the other deactivation pathways. While intersystem crossing is negligible in fluid solvent, it becomes competitive with fluorescence in high viscosity media. The photoisomerization mechanism is discussed on the basis of the model available for stilbene.

### Introduction

Experimental observations have recently established that the unsubstituted stilbene (St) isomerizes in the singlet manifold.<sup>1</sup> The internal rotation about the central double bond (angle  $\vartheta$ ) is an activated process which competes with fluorescence emission from the planar trans configuration while  $S_1 \rightarrow T_1$  intersystem crossing (ISC) has a very low efficiency, at least in inert nonviscous solvent.<sup>1,2</sup> On the basis of theoretical predictions,<sup>3</sup> the rotation leads to a crossing from the lowest excited ( ${}^1B_u$ ) state to a doubly excited ( ${}^1A_g$ ) state.<sup>4</sup> The latter exhibits a potential energy minimum near the perpendicular (perp) configuration from which fast internal conversion (IC) to the maximum of the  $S_0$  curve and decay to its trans and cis sides takes place.

Steric crowding in the vicinity of the ethylenic bridge of St noticeably affects the photophysical and photochemical behavior of the trans isomer which becomes similar to that of the cis isomer due to the common property of inhibited coplanarity caused by the substituents. Steric interaction of the ortho hydrogens with the substituted ethylenic bridge is relieved by twisting about

the exocyclic single bonds.<sup>5</sup> This induces changes in the potential energy profile for twisting about the  $\alpha$ - $\alpha'$  central double bond thus affecting the rate for geometrical photoconversion. In particular, the fluorescence and direct photoisomerization quantum yields of trans  $\alpha$ -CH<sub>3</sub>St and  $\alpha, \alpha'$ -(CH<sub>3</sub>)<sub>2</sub>St are much less sensitive to viscosity and temperature than are the corresponding parameters of trans St.<sup>6</sup> This indicates that the energy barrier existing in St is drastically reduced in the hindered compounds.

Introduction of a nitrogen atom in the ring remarkably affects the excited state behavior of St.<sup>7</sup> It thus seemed interesting to investigate the effect of  $\alpha$ -CH<sub>3</sub> substitution in the three isomeric styrylpyridines (StP's). The results obtained so far on the fluorescence and photoisomerization of the  $\alpha$ -CH<sub>3</sub> derivatives of StP's and some new results on the temperature effect for the unsubstituted StP's are reported and discussed on the basis of the model available for St.

### Experimental Section

The compounds investigated were synthesized by standard procedures,<sup>8</sup> with the exception of  $\alpha$ -CH<sub>3</sub>-3-StP.